

DTP/94/50  
June 1994

# Angular Correlations and Light Gluinos in Multi-jet Photoproduction at HERA

R. Muñoz-Tapia

*Department of Physics, University of Durham  
Durham DH1 3LE, England*

and

W.J. Stirling

*Departments of Physics and Mathematical Sciences, University of Durham  
Durham DH1 3LE, England*

## Abstract

A study of  $3 + 1$  jet event photoproduction at HERA is presented. We define an angular variable which is sensitive to the topology of the final state jets and is therefore able to discriminate between the different contributing subprocesses, and between QCD and an abelian gluon model. We also investigate the contribution from the direct production of light gluinos to the  $3 + 1$  cross section.

# 1 Introduction

The HERA electron-proton collider provides a unique opportunity to study photoproduction processes at high energy [1]. When the scattering angle of the electron is small, the square of the four-momentum transfer is also small and the exchanged particle can be considered as a quasi-real photon. Such photons interact electromagnetically with leptons and quarks, but also have a hadronic component (*i.e.* quark and gluon constituents) from branching processes such as  $\gamma \rightarrow q\bar{q}$ ,  $\gamma \rightarrow q\bar{q}g$  etc. These two types of photon interactions give rise to what are called ‘direct’ and ‘resolved’ processes respectively. Calculations indicate that for the paradigm hard photoproduction process, the production of two jets, the resolved part gives an important contribution at low and moderate jet transverse momenta [2, 3].

The centre-of-mass energy of photon-proton scattering at HERA – typically of order 200 GeV – is large enough to allow the production of multijet events, *i.e.* events with more than two large  $p_T$  jets in the final state. As at the LEP  $e^+e^-$  collider, these can provide detailed tests of QCD matrix elements, as well as measurements of the strong coupling  $\alpha_s$  from comparing cross sections for the production of different numbers of jets.

In this study, we perform a detailed analysis of the production of  $3 + 1$  large  $p_T$  jet events at HERA.\* We will be interested in the case when all the jet transverse momenta are large, in which case the subprocess centre-of-mass energy is a sizeable fraction of the overall  $\gamma p$  energy and as a result the resolved part of the photon gives a negligible contribution. We therefore restrict ourselves to the subprocesses  $\gamma q, \gamma g \rightarrow (q\bar{q}, qgg, q\bar{q}g, \dots)$ . The idea is to try to perform the same type of QCD matrix-element tests that have been performed using the four-jet sample of jet events at LEP, where the dominant processes are  $\gamma^* \rightarrow q\bar{q}gg, qq\bar{q}\bar{q}$ .

As at LEP, it should be feasible to define angular distributions that help in discriminating the parton composition of the final states. At LEP, these have been used, for example, to distinguish QCD from an abelian gluon theory and also to put bounds on the existence of new light fermion species. This is particularly

---

\*The ‘+1’ refers to the proton remnant jet.

important since light, neutral, coloured fermions, the so-called ‘light gluinos’, have not yet been conclusively ruled out by experiments [4]. There has been some speculation that the contribution of such particles to the QCD  $\beta$ -function would reconcile the measurements of  $\alpha_s$  at low and high energies [5, 6, 7, 8]. Recently, several studies suggesting methods of closing the existing window have been published [9, 10, 11, 12]. At the HERA collider, the  $3 + 1$  cross section is the leading-order cross section for the pair production of such gluinos, and might therefore provide the first direct evidence for their existence.

The  $2 \rightarrow 3$  matrix elements which we use to calculate the  $3 + 1$  jet cross sections give rise, in general, to infra-red and collinear singularities when the final state particles are soft and/or collinear with each other and with the incoming particles. We will regulate these in the standard way by requiring that the transverse momenta of the final-state particles (jets) exceeds a certain cutoff  $P_T^{\min}$ , and by requiring a minimum  $\Delta r = (\Delta\eta^2 + \Delta\phi^2)^{1/2}$  separation in the pseudorapidity-azimuthal plane  $(\eta, \phi)$  [13]. This way of defining jet final states has already been used successfully at HERA [14]. The maximum pseudorapidity of each jet is also restricted, to keep the jets away from the beam direction.

In the following section we describe the general features of the  $3 + 1$  jet cross section, and calculate the contributions to the total cross section from the different subprocesses. In Section 3 we introduce an angle which characterizes the topology of the final state and which can, in principle, discriminate between the different subprocesses. In Section 4 we discuss a possible ‘light gluino’ contribution to the cross section, and in Section 5 we present our conclusions.

## 2 The total $3 + 1$ jet cross section

The total cross section for a  $3 + 1$  jets final state can be written schematically as

$$\sigma(ep \longrightarrow e + 3\text{jets} + X) = \sum_{a, c_i=q,g} G_{\gamma/e} * G_{a/p} * \hat{\sigma}(\gamma a \rightarrow c_1 c_2 c_3), \quad (1)$$

where  $G_{\gamma/e}$  and  $G_{a/p}$  denote the photon content of the electron and the parton content of the proton respectively. For the latter, we use the MRS(D’<sub>0</sub>) set [15],

although none the quantities that we will calculate will be particularly sensitive to this choice – our quarks and gluons will be probed at relatively large  $x$  where they are well constrained by deep inelastic and other data. The symbol  $*$  denotes a convolution operation and  $\hat{\sigma}$  refers to the partonic cross sections of the relevant processes. The  $Q^2$  scale in the parton distributions and in the strong coupling constants in the subprocess cross sections is set equal to the minimum jet transverse momentum in each event. To a very high accuracy the Weizsäcker-Williams approximation [16] (already implicit in Eq. (1)) can be used for the photon content of the electron [17]

$$G_{\gamma/e} = \frac{\alpha}{2\pi} \log\left(\frac{s}{4m^2}\right) \frac{1 + (1-x)^2}{x}, \quad (2)$$

where  $\alpha$  is the electromagnetic coupling constant,  $s$  is the centre-of-mass energy squared, and  $x$  is the fraction of energy lost by the electron  $x = (E - E')/E$ . In a recent paper Frixione *et al.* [18] have studied the validity of the approximation (see also [19]). The sub-leading corrections are negative, indicating that the above approximation always overestimates the cross section. None of our results, however, depend sensitively on the absolute size of our cross sections.

In Fig. 1 we show the total cross section for the process  $e + p \rightarrow e + 3 \text{ jets} + X$  as a function of the minimum transverse momentum cut  $P_T^{\min}$ . The contributions of the different subprocesses are also shown. We have set the cut-off  $\Delta r^{\min}$  of the jet-defining algorithm to 1.0, in accordance with Ref. [20], and the maximum rapidity of the jets (in the  $\gamma p$  centre-of-mass frame) is 2.0. Notice that the 2 quark + 1 gluon configuration dominates at low  $P_T^{\min}$ . This contribution is proportional to the gluon distribution in the proton, which at small  $x$  (*i.e.* small  $P_T^{\min}$ ) is larger than the quark distributions. At large  $P_T^{\min}$ , on the other hand, the partons are probed at large  $x$  and the quark-induced subprocesses dominate. The crossing between the two occurs at around  $P_T^{\min} = 25 \text{ GeV}/c$ .

### 3 Angular distributions

Angular variables for multijet final states have long been used in  $e^+e^-$  colliders, see for example Ref. [21]. Due to their different helicity and colour properties,

quarks and gluons exhibit different behaviour in certain kinematic variables. This fact can be used to discriminate the parton content of the final-state jets. For example, for  $e^+e^- \rightarrow 4$  jets the modified Nachtmann-Reiter angle and the azimuthal angle between the planes defined by the two final-state jet pairs have led to important tests of the QCD structure of the matrix elements [22].

Here we attempt to define an analogous angular variable which is suited to the study of  $3 + 1$  jet final states at the HERA  $ep$  collider.<sup>†</sup> First, the jets are ordered according to their transverse momentum  $P_T$ . Then the angle  $\theta_H$  between the planes formed by the highest  $P_T$  jet and the beam and the plane formed by the other two jets is computed. In addition, we require the highest  $P_T$  jet to be central in rapidity, so that the typical configuration is that of an energetic jet in one hemisphere balanced by two less energetic jets in the opposite hemisphere.

One important difference between LEP and HERA is that only for the former do the lab and multijet centre-of-mass frames coincide. Any information about the angular correlations between the final-state partons at HERA tends to be smeared out in going from the parton subprocess frame to the lab frame. In order to understand the underlying QCD physics, therefore, we first analyse the angular distribution in the subprocess centre-of-mass frame.

We first consider the angular distributions between the final states *without* a central rapidity cut on the highest  $P_T$  jet. In this case we find that the  $1$  quark +  $2$  gluons final state ( $\gamma q \rightarrow qgg$ ) shows a qualitatively different behaviour to the other two processes. For this process we would expect the quark to be the most energetic particle because of the infra-red singularities for soft gluon emission. (This is analogous to the  $q\bar{q}gg$  final state at LEP where the gluons are generally the softest jets.) The distribution in the polar angle formed by the beam direction and the quark jet is fairly flat, having a broad peak around  $90^\circ$  and decreasing at  $0^\circ$  and  $180^\circ$  due to the rapidity and  $P_T^{\min}$  cuts. However in the  $3$  quarks final state ( $\gamma q \rightarrow qq\bar{q}$ ), the highest  $P_T$  jet has a distribution of the angle with the beam direction peaked at low angles. This difference can be understood as follows. In the first case, diagrams involving the trilinear gluon coupling give an important

---

<sup>†</sup>We assume in what follows that a sufficiently large sample of such events will be collected over the lifetime of the machine in order to perform such a study.

contribution and the subprocess scattering is effectively  $\gamma q \rightarrow qq^*(\rightarrow gg)$ , with  $t$ -channel fermion exchange at small angles. In the second case, the dominant configuration is effectively  $\gamma \rightarrow q\bar{q}$  followed by  $qq \rightarrow qq$ , which proceeds via  $t$ -channel gluon exchange and is therefore more peaked at small angles. The 2 quark+1 gluon final state process ( $\gamma g \rightarrow q\bar{q}g$ ) shows a distribution in polar angle of the largest  $P_T$  jet similar to that of the 3 quark final state. Here, again, the dominant configuration involves an initial state  $\gamma \rightarrow q\bar{q}$  splitting followed by  $gg \rightarrow gg$  involving  $t$ -channel gluon exchange.

Now since we are interested in increasing the sensitivity to the triple-gluon vertex in *final-state* gluon radiation, as at LEP, it is sensible to require the fastest  $P_T$  jet to be central in rapidity, thus suppressing processes involving *initial-state* splitting, like the second and third type discussed above.

In Fig. 2 we show the total cross section for the 3+1 process in the HERA frame when the central cut  $|\eta| < 0.5$  for the largest  $P_T$  jet is included. Note that the overall decrease in rate compared to Fig. 1 is not particularly significant.

In Fig. 3 the distributions in the angle  $\theta_H$  – in the subprocess centre-of-mass frame – are presented for the sum of all processes, and for each subprocess normalized separately. As we had anticipated, there is a distinct difference in the distributions depending on the composition of the final-state jets. The planes corresponding to the 1 quark + 2 gluon final state tend to be aligned perpendicularly ( $\theta_H \sim 90^\circ$ ) while the other two processes show a peak at low angles. This can be understood as follows. When the beam direction is coplanar with the 3 quark (or 2 quark + 1 gluon) final state, the important  $t$ -channel gluon exchange contribution is maximized, thus favouring low  $\theta_H$ . However, in the 1 quark + 2 gluon final state case the pole structure is milder and other kinematic effects come into play. The two gluons are expected to end up as the softest jets, whereupon they define one of the planes for computing  $\theta_H$ . For these two jets, the rapidity and  $P_T$  cuts have a bigger impact, and the number of events with the beam direction perpendicular to the plane of the final-state jets is enhanced.

In order to distinguish kinematic and dynamical effects, it is useful to compare the QCD angular distributions with those of a phase-space model, where the matrix elements are constant. In Fig. 4 the phase space  $\theta_H$  distribution is

compared with the distribution for the QCD 1 quark + 2 gluons final state, and also with that of an ‘abelian’ QCD model [23], *i.e.* a  $U(1)_3$  gauge theory with a coupling constant  $\alpha_{ABE} = 4/3\alpha_s$  chosen to compensate the QCD  $q \rightarrow qg$  colour factor. This model provides a useful benchmark for demonstrating sensitivity to the triple-gluon vertex. We see from Fig. 4 that the abelian and phase-space distributions have roughly the same shape, both showing a small peak at low angles and a decrease at higher angles, in contrast to the QCD result which is peaked at high angles. The decrease of the phase space distribution is due to the angular dependence introduced by the  $P_T$  ordering – without this ordering the distribution would be essentially flat. Notice that the configuration of the final jets produced in the phase-space model is different to that of the QCD 1 quark + 2 gluons subprocess, where, on average, two of the jets are significantly softer than the third. This explains why the cuts have a different effect in the two cases. This distinctive behaviour gradually disappears as the  $P_T^{\min}$  cut is increased above 20 GeV, when most the events at low  $\theta_H$  are removed.

We next consider the  $\theta_H$  distribution in the HERA lab frame. The boost induced by the more energetic proton beam squeezes the difference between distributions into a smaller part of the angular range. In addition, there is a greater sensitivity to the jet rapidity cuts.<sup>‡</sup> Figure 5 shows the same distributions in Fig. 3 but now in the HERA frame. Again, we see that the distribution for the 1 quark + 2 gluons final state is larger for higher angles, while the distributions for the other processes decrease at higher angles. Although the effect is less pronounced than in the centre-of-mass frame, the distributions still show differences of order 50% at perpendicular angles. The main problem here is that the pattern of each curve starts to be distinctive only from about  $60^\circ$  onwards. The comparison of the QCD 1 quark + 2 gluons process with the abelian and phase-space models is shown in Fig. 6. The differences in shape again only start to be noticeable at higher angles, because most of the events at low angles have been boosted out of the rapidity acceptance.

---

<sup>‡</sup>To compensate for this, we increase  $|\eta|_{\max}$  from 2.0 to 3.0 in what follows.

## 4 Light gluino production

The production of  $3 + 1$  jets at HERA is the leading process for the pair production of gluinos:  $\gamma q \rightarrow q\tilde{g}\tilde{g}$ . In a previous study [24], we analysed the angular correlations in 4-jet production at LEP to investigate the effect of light gluino pairs in the final state. Here we do the same for  $3 + 1$  jet production at HERA. As an application of the shape distributions introduced in the previous section, one can study the influence of a light gluino particle. Note that other methods of detecting light gluinos at HERA, in particular through their effect on deep inelastic structure functions, have been shown to be very difficult [25, 26].

In Fig. 7 we show the predicted total cross section for the photoproduction of gluino pairs in  $3 + 1$  jet events as a function of  $P_T^{\min}$ , compared with the QCD result. Since there is a difference of almost two orders of magnitude between the two, it will be practically impossible to detect any effect from the total cross section alone.

In Fig. 8 the  $\theta_H$  distribution for gluino photoproduction in the partonic centre-of-mass and HERA frames is shown. Notice that the shape is very similar to that of the  $1$  quark +  $2$  gluon final state. The Feynman diagrams contributing to gluino-pair production coincide with those containing the triple-gluon vertex in the  $qgg$  case. The same arguments given in the previous section apply here, and so the plane formed by the light gluinos will be preferentially oriented perpendicular to the direction of the beam. However, the difference in shape is not big enough to compensate for the overall smallness of the gluino contribution, as shown in Fig. 8. The only hope will be to look for the decay signature of a colourless glueballino ( $g\tilde{g}$ ) formed after the hadronization process, as suggested in Refs. [11, 12]. If enough events are produced, the angular distribution could be used to perform a further test.

## 5 Conclusions

In this paper we have studied the photoproduction of  $3 + 1$  jet events at the HERA  $ep$  collider. An angular variable, defined in terms of the directions of the



final-state jets, has been shown to discriminate between the different types of contributing subprocess. This can be used to check the parton composition of the final-state jets, to verify that QCD is favoured over phase-space and abelian gluon models, and to put bounds on new light particle species. In particular, we have studied the influence of a light gluino, whose existence is still controversial. Only a very small modification on the angular distribution is expected.

## Acknowledgements

We are grateful to Tim Stelzer for discussions and for providing us with the MADGRAPH [27] program for computing the matrix elements. Useful discussions with Valery Khoze are also gratefully acknowledged. This research is supported in part by the Commission of the European Communities ‘Human Capital and Mobility’ Network contract CHRX-CT92-0004 and (RMT) contract ERB4001GT921106.

## References

- [1] G.A. Schuler, in Proc. of the Workshop *Physics at HERA* (1992), Vol.1, p.461, eds. W. Buchmüller and G. Ingelman, DESY 93-01.
- [2] W.J. Stirling and Z. Kunszt, in Proc. of DESY Workshop on *Physics at HERA* (1987), Vol.1, p.331, ed. R.D. Peccei.
- [3] H1 collaboration, T. Ahmed *et al.*, Phys. Lett. **297B** (1992) 205; ZEUS collaboration, M. Derrick *et al.*, Phys. Lett. **297B** (1992) 404.
- [4] UA1 collaboration, C. Albajar *et al.*, Phys. Lett. **198B** (1987) 261; Phys. Rev. Lett. **62** (1989) 1825.
- [5] I. Antoniadis, J. Ellis and D.V. Nanopoulos, Phys. Lett. **262B** (1991) 109.
- [6] M. Jezabek and J.H. Kuhn, Phys. Lett. **301B** (1993) 121.
- [7] J. Ellis, D.V. Nanopoulos and D.A. Ross, Phys. Lett. **305B** (1993) 375.

- [8] M. Carena and L. Clavelli, Phys. Lett. **317B** (1993) 346.
- [9] J.I. Lopez, D.V. Nanopoulos and X. Wang, Phys. Lett. **313B** (1993) 241.
- [10] C. Bhattachayya and A. Raychaudhuri, Phys. Rev. **D49** (1994) 1156.
- [11] F. Cuypers, Phys. Rev. **D49** (1994) 3075.
- [12] C.E. Carlson and M.Sher, Phys. Rev. Lett. **72** (1994) 2686.
- [13] UA1 collaboration, G. Arnison *et al.*, Phys. Lett. **123B** (1983) 115; *ibid.* **132B** (1983) 214.
- [14] V. Hedberg *et al.*, “Study of jet reconstruction algorithms for HERA *ep* collider events”, preprint DESY 93-190, December 1993.
- [15] A.D. Martin, W.J. Stirling and R.G. Roberts, Phys. Lett. **306B** (1993) 145; err. *ibid.* **B309** (1993) 492.
- [16] C.F. Weizsäcker, Zeit. f. Phys. **88** (1934) 612; E.J. Williams, Phys. Rev. **45** (1934) 729.
- [17] Min-Shih Chen and P.M. Zerwas, Phys. Rev. **D12** (1975) 187.
- [18] S. Frixione *et al.*, Phys. Lett. **319B** (1993) 339.
- [19] A.I. Lebedev, in Proc. of the Workshop *Physics at HERA* (1992), Vol.1, p.613, eds. W. Buchmüller and G. Ingelman, DESY 93-01.
- [20] J.E. Huth *et al.*, in Proc. of the 1990 *DPF Summer Study on High Energy Physics*, Snowmass, Colorado, p.134, ed. E.L. Berger (World Scientific, Singapore 1992).
- [21] T. Hebbeker, Phys. Rep. **217** (1992) 69.
- [22] O. Nachtmann and A. Reiter, Zeit. f. Phys. **C 16** (1982) 45; M. Bengtsson, Zeit. f. Phys. **C 42** (1989) 75.
- [23] S. Bethke, A. Ricker and P.M. Zerwas, Zeit. f. Phys. **C 49** (1991) 59.

- [24] R. Muñoz-Tapia and W.J. Stirling, Phys. Rev. **D49** (1994) 3763.
- [25] R.G. Roberts and W.J. Stirling, Phys. Lett. **313B** (1993) 453.
- [26] J. Blümlein and J. Botts, Phys. Lett. **325B** (1994) 190.
- [27] T. Stelzer and W.F. Long, “Automatic generation of tree level helicity amplitudes”, University of Wisconsin preprint MAD-PH-813 (1994).

## Figure captions

- [1] Total cross section for the process  $e + p \rightarrow e + 3 \text{ jets} + X$  as a function of the minimum jet transverse momentum cut  $P_T^{\min}$ . The UA1 jet algorithm is used with  $\Delta r^{\min} = 1.0$ . The maximum jet pseudorapidity is  $|\eta|_{\max} = 2.0$ . The solid line corresponds to the total cross section, summed over all subprocesses. The dashed, dotted, and dash-dotted lines show the contributions from the 1 quark + 2 gluons, 2 quarks + 1 gluon, and 3 quarks final states respectively.
  
- [2] Total cross section for the process  $e + p \rightarrow e + 3 \text{ jets} + X$  as a function of the minimum jet transverse momentum cut  $P_T^{\min}$ , when a central cut  $|\eta| \leq 0.5$  on the highest  $P_T$  jet is included and  $|\eta|_{\max} = 3.0$ . The solid line corresponds to the total cross section, summed over all subprocesses. The dashed, dotted, and dash-dotted lines show the contributions from the 1 quark + 2 gluons, 2 quarks + 1 gluon, and 3 quarks final states respectively.
  
- [3] Shape distribution in the angular variable  $\theta_H$ , defined in the text, for the three-jet subprocesses in the centre-of-mass frame of the photon-parton subsystem. In the 3-quark final state the mass of the  $b$  quark has been taken into account. The highest  $P_T$  jet is required to be central by imposing a cut pseudorapidity,  $|\eta| \leq 0.5$ . The solid line corresponds to the sum over all processes. Note that each line has been normalized separately to unit area.
  
- [4] Shape distribution in the angular variable  $\theta_H$  for the 1 quark + 2 gluons QCD subprocess, and the same subprocess in an abelian model, in the photon-parton centre-of-mass frame. The dashed line shows the distribution corresponding to the phase-space model. A cut on the highest  $P_T$  jet,  $|\eta| \leq 0.5$ , is also imposed.
  
- [5] Shape distribution in the angular variable  $\theta_H$  for the three-jet subprocesses in the HERA lab frame. The maximum pseudorapidity is now  $|\eta|_{\max} = 3.0$ . The dashed, dotted, and dash-dotted lines show the distributions for the 1

quark + 2 gluons, 2 quark + 1 gluon, and 3 quarks final states respectively. The solid line corresponds to the sum over all processes.

- [6] Shape distribution in the angular variable  $\theta_H$  for the 1 quark + 2 gluons QCD subprocess, and the same subprocess in an abelian model, in the HERA lab frame. The dashed line shows the phase-space model distribution.
- [7] The total cross section for the process  $e + p \rightarrow e + 3 \text{ jets} + X$  compared to  $e + p \rightarrow e + q + \tilde{g}\tilde{g} + X$  as a function of the minimum jet transverse momentum  $P_T^{\min}$ , for  $m_{\tilde{g}} = 5 \text{ GeV}/c^2$ .
- [8] Comparison of the  $\theta_H$  shape distribution for the total 3-jet cross section and for the contribution from a light ( $m_{\tilde{g}} = 5 \text{ GeV}/c^2$ ) gluino. The dash-dotted, solid and dashed lines show the gluino, 3-jet QCD and combined distributions respectively (a) in the photon-parton centre-of-mass frame, and (b) in the HERA lab frame.

This figure "fig1-1.png" is available in "png" format from:

<http://arXiv.org/ps/hep-ph/9407225v1>

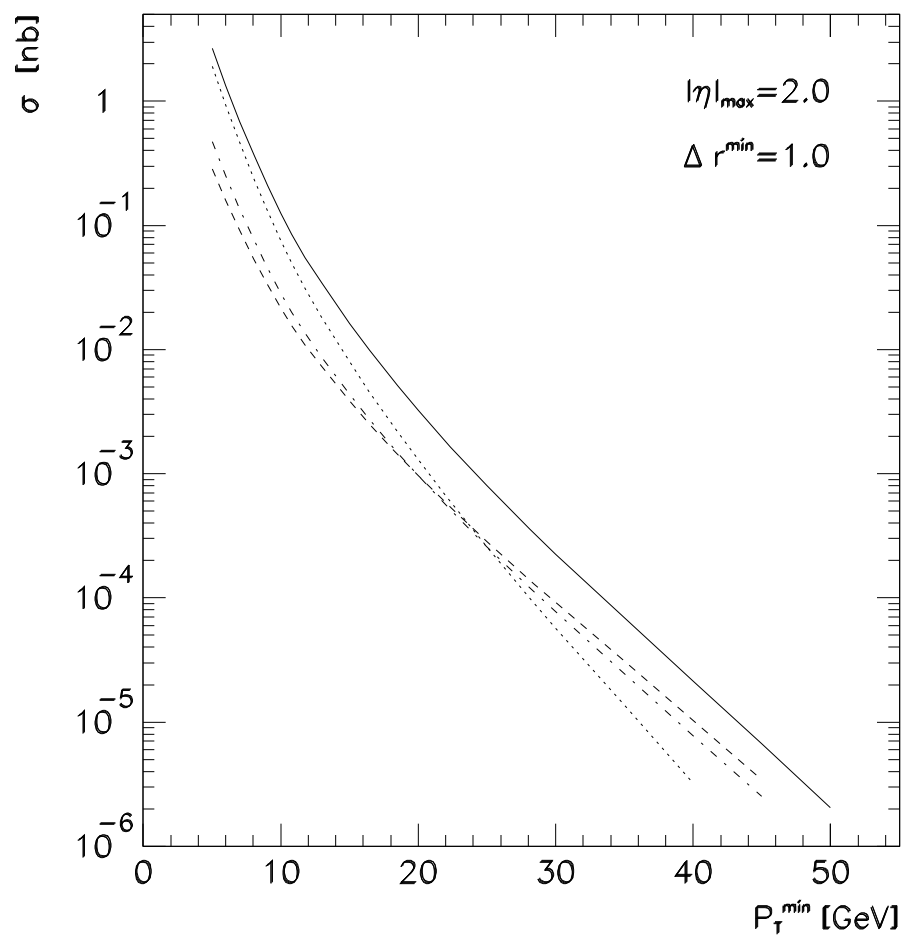


Fig. 1

This figure "fig2-1.png" is available in "png" format from:

<http://arXiv.org/ps/hep-ph/9407225v1>



This figure "fig1-2.png" is available in "png" format from:

<http://arXiv.org/ps/hep-ph/9407225v1>

This figure "fig2-2.png" is available in "png" format from:

<http://arXiv.org/ps/hep-ph/9407225v1>

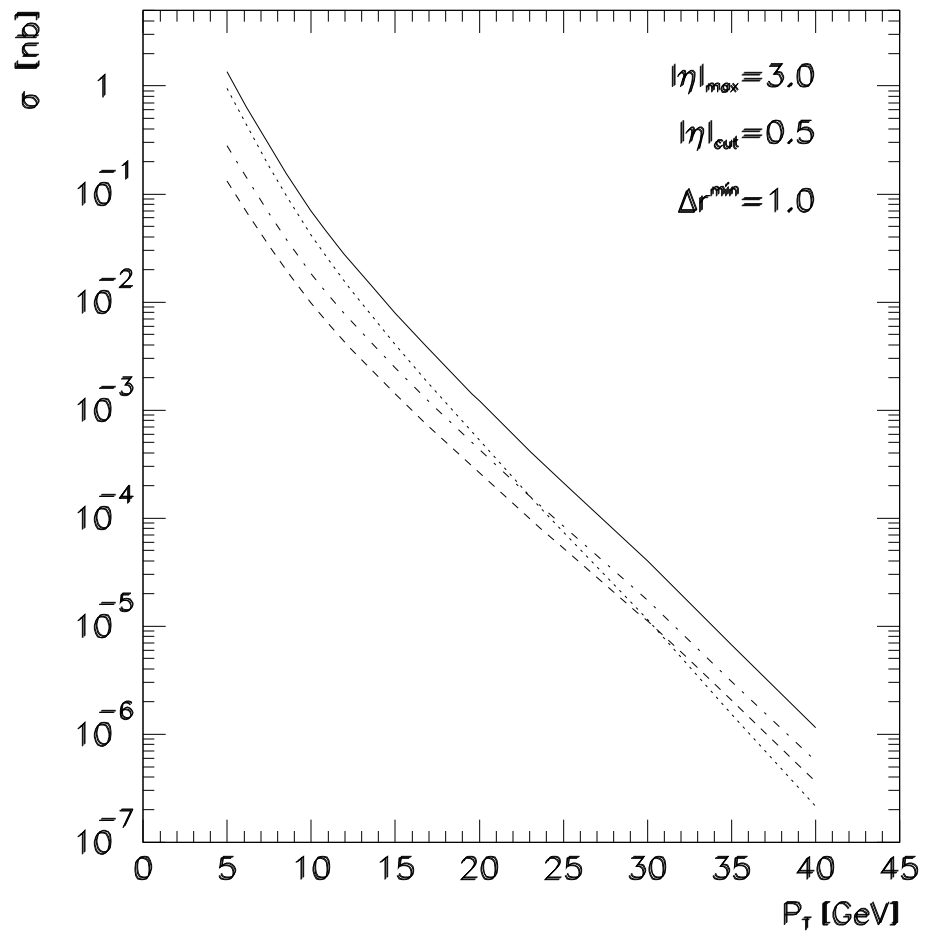


Fig. 2

This figure "fig1-3.png" is available in "png" format from:

<http://arXiv.org/ps/hep-ph/9407225v1>

This figure "fig2-3.png" is available in "png" format from:

<http://arXiv.org/ps/hep-ph/9407225v1>

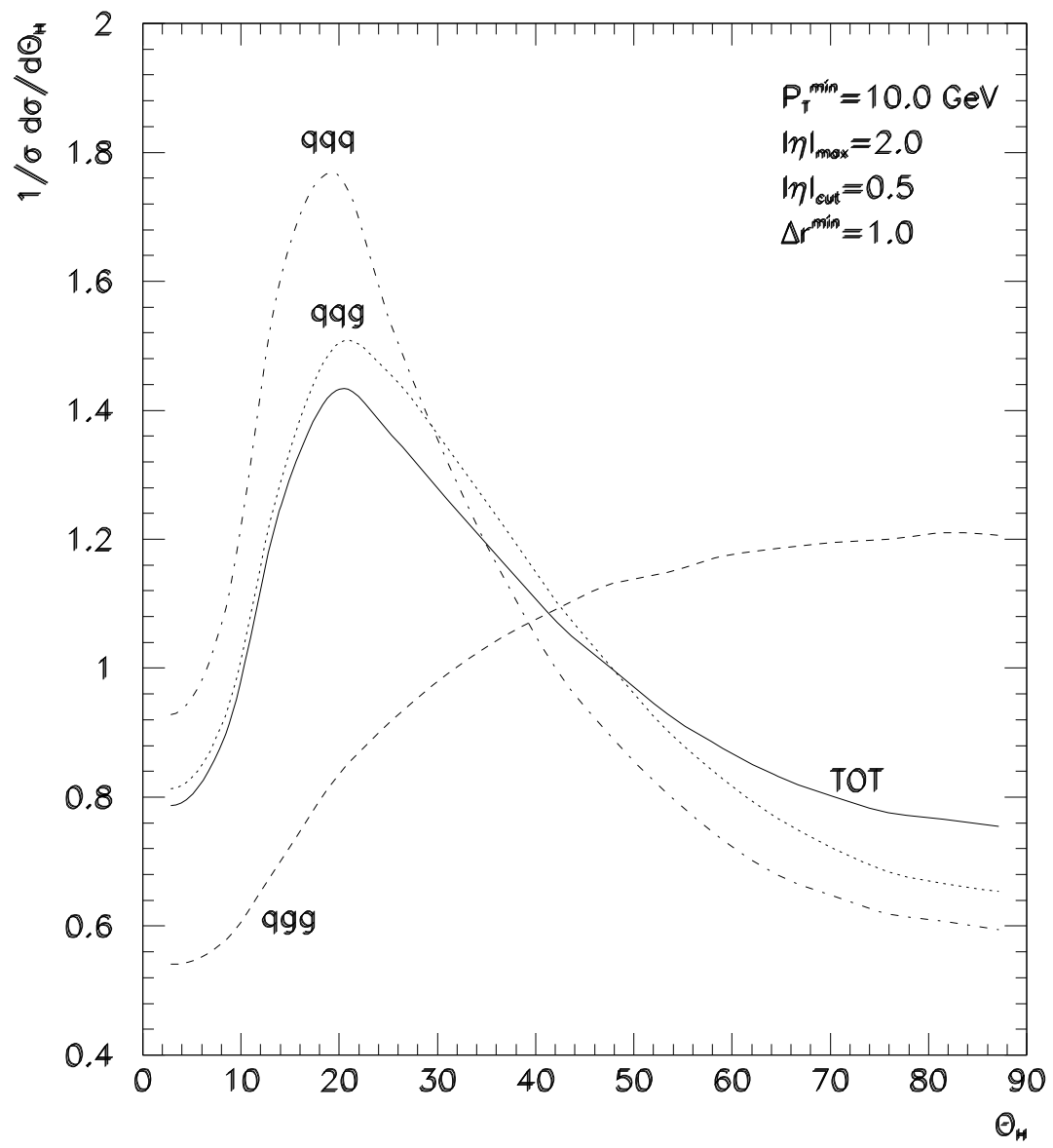


Fig. 3

This figure "fig1-4.png" is available in "png" format from:

<http://arXiv.org/ps/hep-ph/9407225v1>

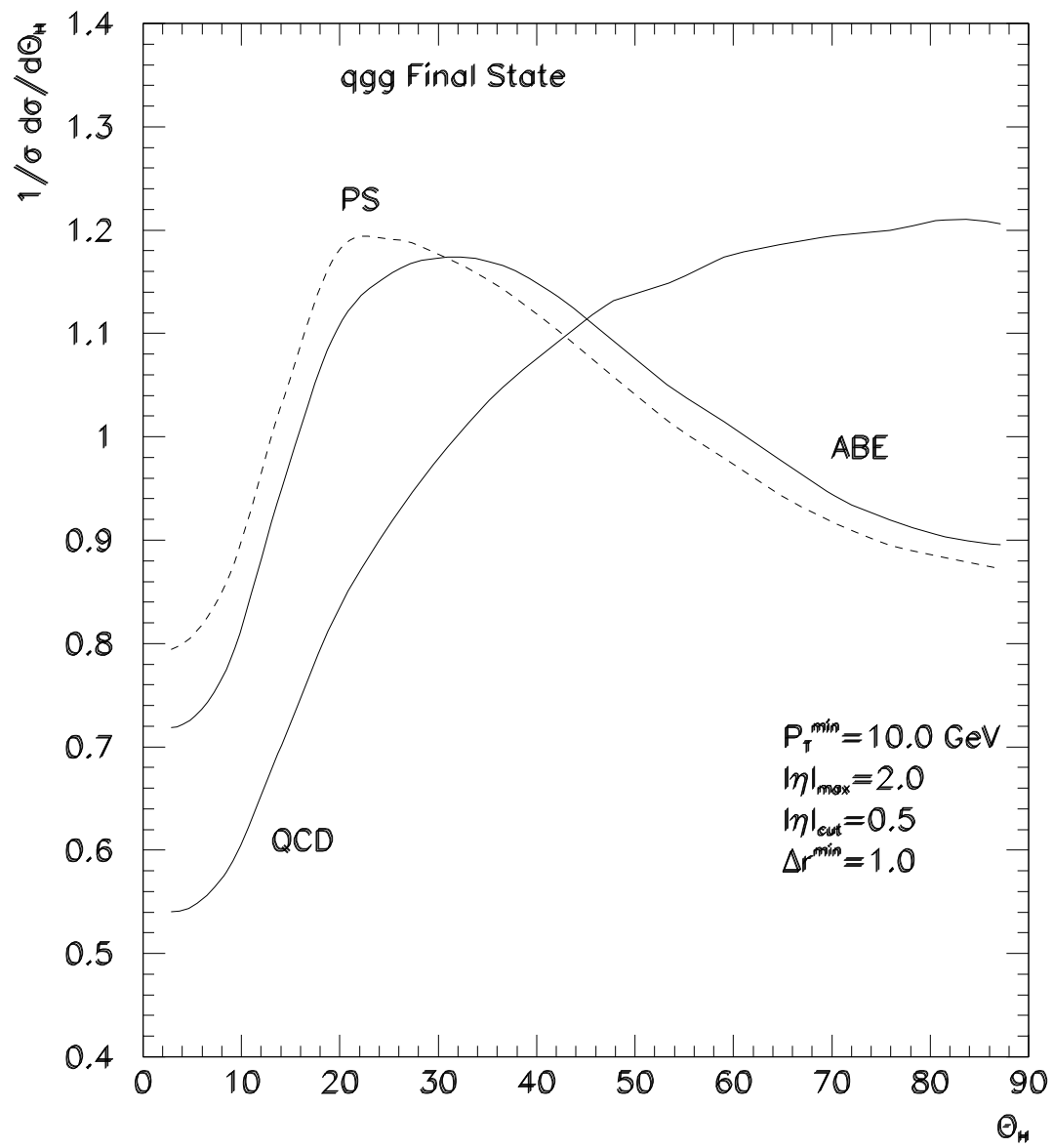


Fig. 4



This figure "fig1-5.png" is available in "png" format from:

<http://arXiv.org/ps/hep-ph/9407225v1>

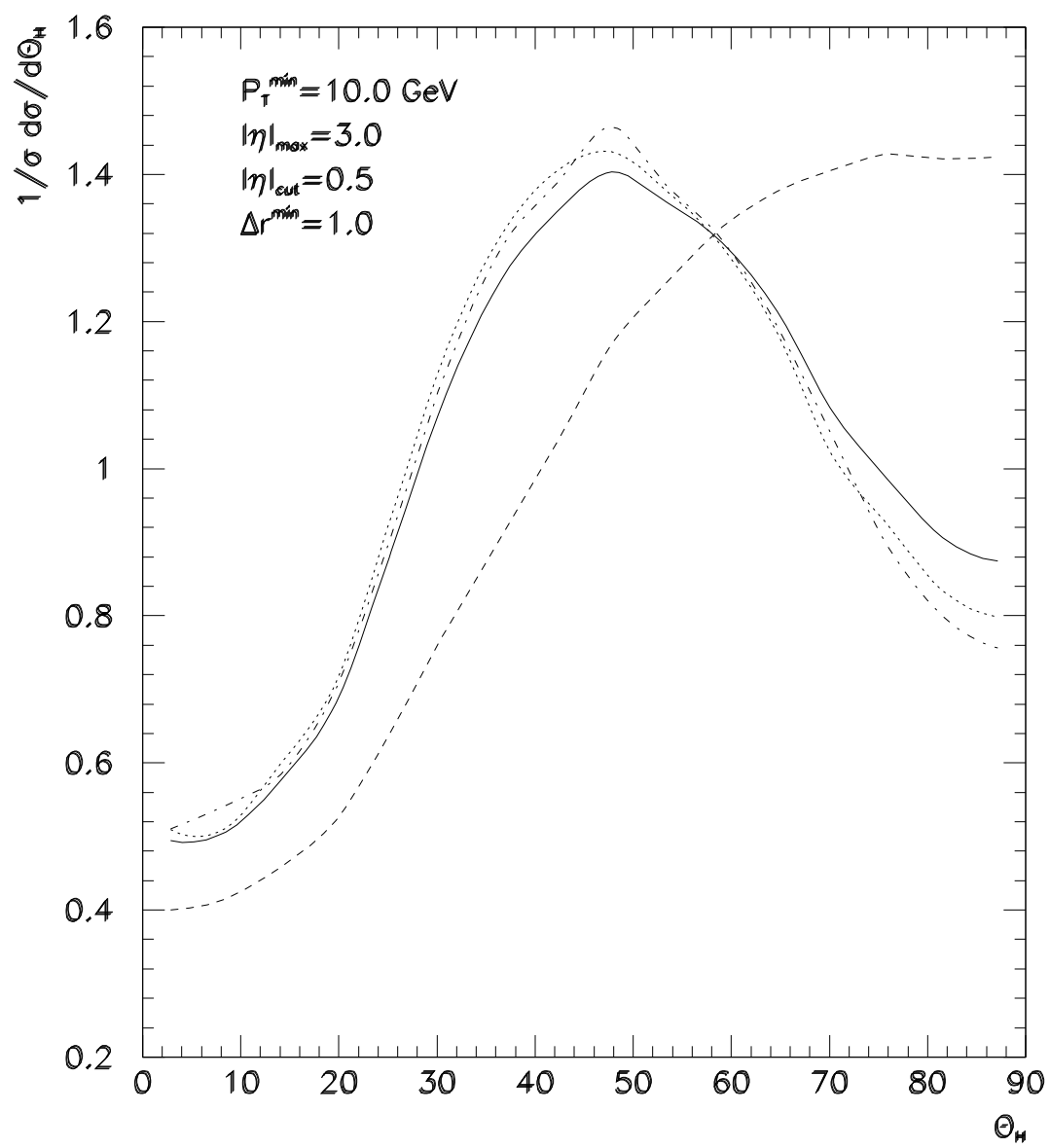


Fig. 5

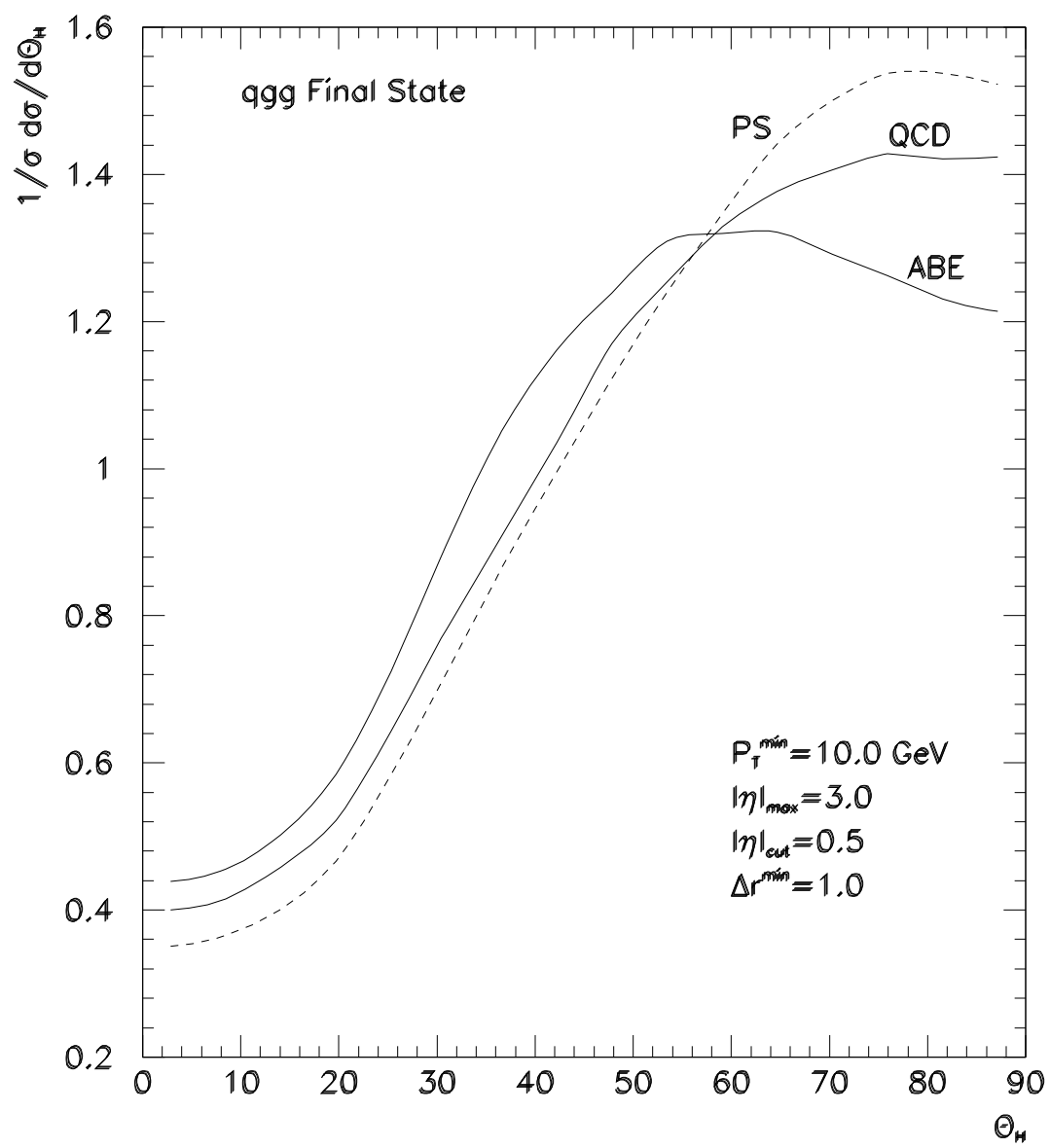


Fig. 6

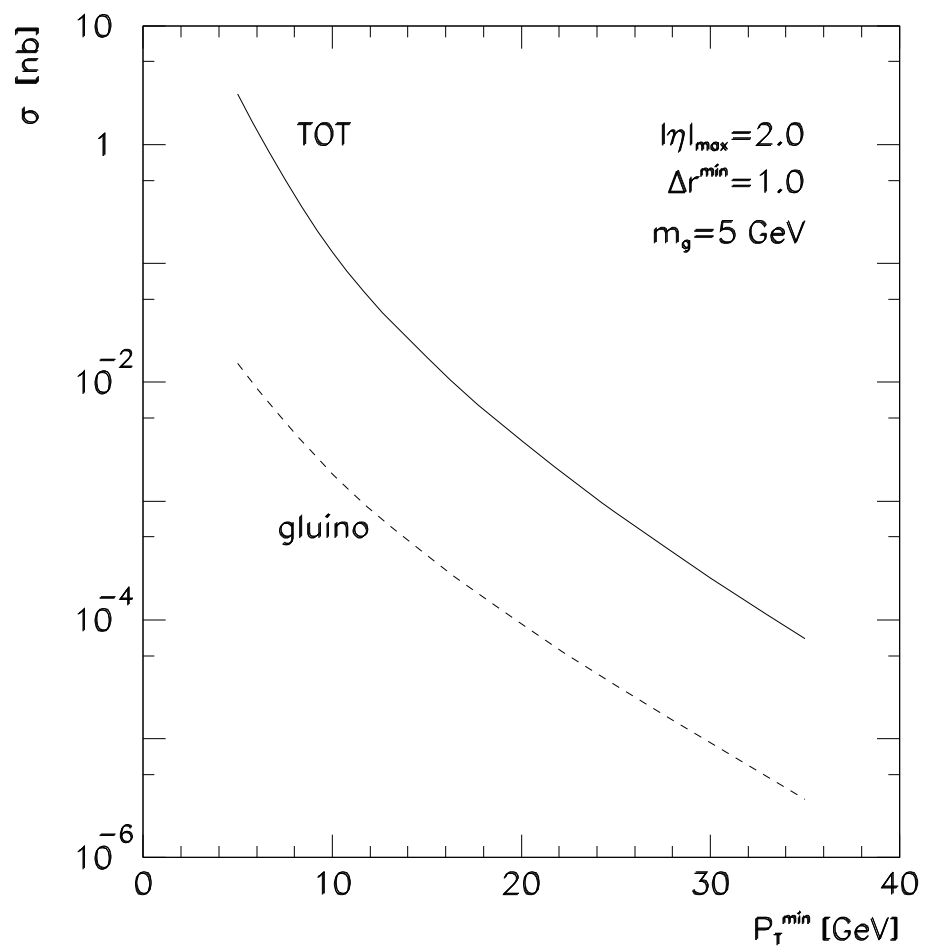


Fig. 7

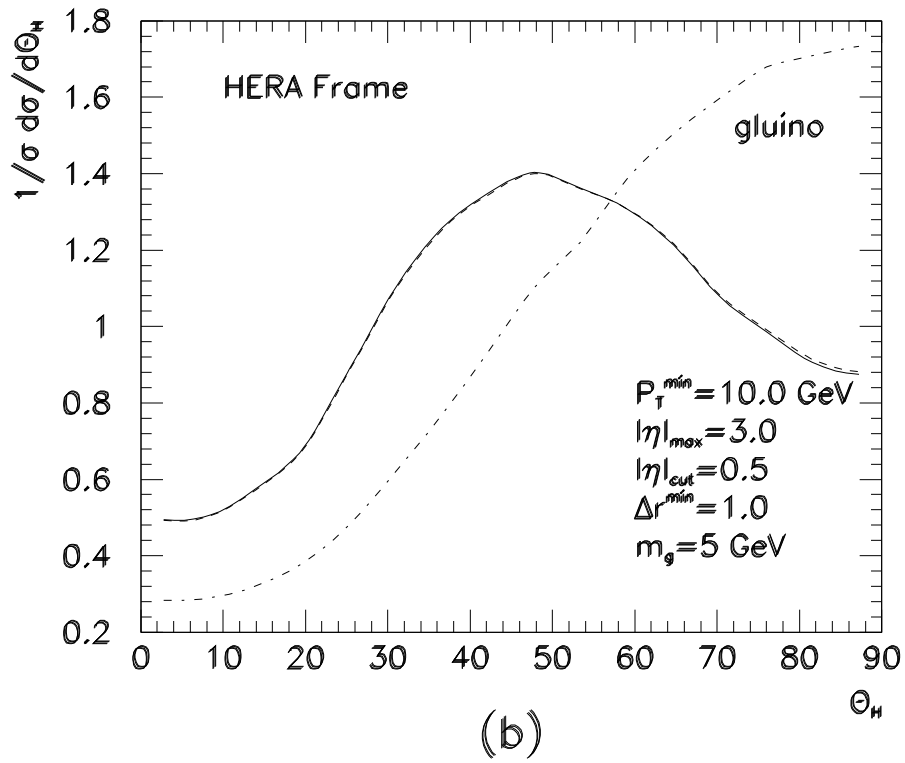
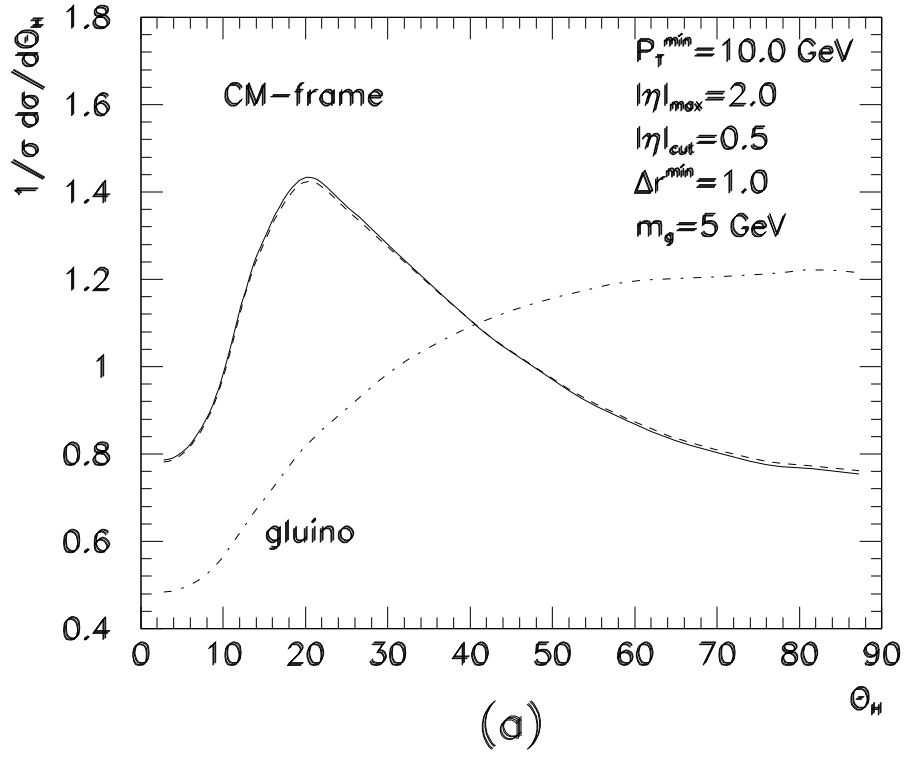


Fig 8